Tracking mixing by overturning internal waves

Philippe Odier, Yvan Dossmann, Baptiste Bourget, Christophe Brouzet, Sylvain Joubaud and Thierry Dauxois

Univ Lyon, ENS de Lyon, Univ Claude Bernard, CNRS
Laboratoire de Physique, F-69342 Lyon, FRANCE
philippe.odier@ens-lyon.fr

Abstract

We present a novel characterization of mixing events associated with the propagation and overturning of internal waves, studied thanks to the simultaneous use of Particle Image Velocimetry (PIV) and Planar Laser Induced Fluorescence (PLIF) techniques, which are applied for the first time to the case of a continuous stratification. A precise measurement of the turbulent diffusivity K_t associated with mixing events induced by an internal wave mode is performed. Values up to $K_\mathrm{t} = 15\ \mathrm{mm}^2 \cdot \mathrm{s}^{-1}$ are reached when the wave is unstable under Triadic Resonant Interaction (TRI), unambiguously confirming that TRI is a potential pathway to turbulent mixing in stratified flows. This work therefore provides a step on the path to new measurements for internal waves.

1 Introduction

Internal waves are ubiquitous in the ocean, due to the stratification in temperature and salinity. They are generated either from the interaction of tidal currents with submarine bathymetry (Garrett and Kunze, 2007), or by wind stress at the ocean surface (Munk and Wunsch, 1998). They can travel long distances, to reach places where they dissipate via various breaking mechanism (Staquet and Sommeria, 2002). In the dissipation processes, they can produce mixing of the local stratification. These mixing processes are still scarcely understood, since in numerical simulations, they take place at sub-grid scales, while in-situ measurements can only provide a discrete sampling of oceanic regions (although breaking internal waves have been observed in the ocean, see Lamb (2014) for a review). It is important to understand the mixing due to internal waves, since it could be one of the mechanisms to convert kinetic energy into potential energy, to maintain the ocean stratification against the tendency of settling more and more denser water at the bottom, via gravity currents (Kunze and Smith, 2004; Wunsch and Ferrari, 2004).

A direct characterization of mixing events would involve, for example, a detailed measurement of the vertical buoyancy flux, $g\,\langle \rho' w' \rangle / \overline{\rho}$, induced by the waves, where $\overline{\rho}$ is the average density, g the gravity acceleration, ρ' and w' the fluctuating parts of the density and vertical velocity fields, while $\langle \cdot \rangle$ indicates ensemble- or time-averaging. In order to measure this quantity, a simultaneous quantitative measurement of the velocity and density fields in a continuous stratification is necessary. PIV is a very convenient technique to measure the velocity field and it can be combined with Planar Laser Induced Fluorescence (PLIF) that gives access to the density field. However, PLIF has never been used quantitatively in the case of continuous stratification, due to the low signal/noise ratio that this implies, compared to its current use in two-layer systems, such as jets (Hu et al., 2000), wakes (Hjertager et al., 2003), gravity currents (Odier et al., 2014) or interfacial waves (Troy and Koseff, 2005). In this article, we show that the PIV/PLIF technique can also be used for continuous stratification to assess mixing-related quantities in the context of internal gravity waves.

2 Experimental set-up

Experiments are conducted in a 80 cm long, 17 cm wide rectangular tank. It is filled to a height of 32 cm with a linearly stratified fluid of density $\rho(z)$. Stratification is controlled using salt and ethanol, this combination allowing to keep a constant refraction index throughout the tank volume, while providing a linear stratification. The tank is also linearly stratified in Rhodamine 6G, to produce the PLIF signal. The buoyancy frequency $N = (-g\partial_z\rho/\overline{\rho})^{1/2}$ is about 1 rad·s^{-1}. A periodic internal wave is generated using a wave generator (Gostiaux et al., 2007) placed vertically on a side of the tank. A mode-1 wave configuration propagating from left to right is forced (see schematics of the experimental set-up in Fig. 1). The generator forcing frequency is imposed using a Labview program.

Images are recorded with two CCD Allied Vision Pike cameras, 14-bits, 2452×2054 pixels, placed at 280 cm from the tank. The cameras are mounted with a 35 mm lens, producing a 40 cm by 60 cm field of view. An optical filter (high-pass in wavelength, cut-off 550 nm), is placed in front of the PLIF camera to allow only for the fluorescence light and to block the laser scattered light. For the PIV camera, a band-pass optical filter (530 ± 5 nm), blocks the fluorescence light while passing the laser light, scattered by PIV particles seeded in the tank. The two cameras are synchronized spatially, using a calibration grid, and temporally, using a common trigger signal, to ensure that a given location in the field of view is properly matched between the two images and that the images are taken at the same time. The PIV interrogation window size is 21×21 pixels and the spatial resolution for the velocity field is 2.5 mm, while the spatial resolution for the density field is 0.25 mm. If necessary, it can be coarse-grained to match the PIV resolution.

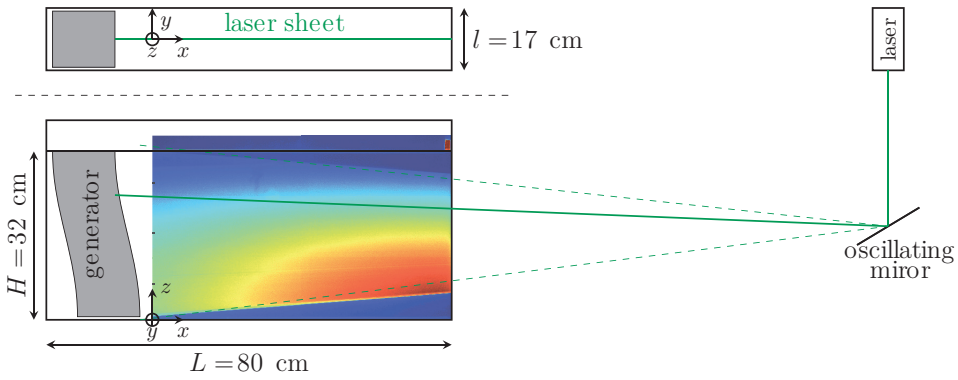

Figure 1: The top panel presents the top view of the experimental set-up, while the bottom one shows a side view, with a raw image placed as a background. Note that the greyscale of the black and white camera has been replaced by a color scale for vizualisation purposes. The rest position of the front face of the wave generator is located at x =-5 cm.

The PLIF excitation light is produced by a Laser Quantum Ti:Sapphire Opus laser (532 nm), reflected on an oscillating mirror, creating a vertical light sheet, illuminating a vertical cut of the stratified fluid, in the middle of the tank width. The absorption of laser light by the dye (and, to a lesser extent, by the other components of the fluid) creates a decrease of light intensity that can be seen in figure 1, from right to left. This light absorption must be corrected for, in order to allow for quantitative measurements of the density field. The calibration procedure used here is based on the knowledge of images without any wave motion and is then applied iteratively along the ray paths. For more details, see Dossmann et al. (2016).

3 Assessment of mixing processes

The initial goal in applying the coupled PIV/PLIF technique to an internal wave set-up was to be able to characterize the mixing induced by overturning waves. A qualitative picture of such an event can be observed in Fig. 2, showing the superposition of the velocity field measured by PIV (arrows) and of the density field, represented by selected isopycnal (colored lines). The velocity field shows the mode-1 wave rolls, superimposed with regions of more turbulent motion (on the left). The isopycnals illustrate local overturn events, coinciding with the turbulent regions of the velocity field. In these regions, the combination of these overturn events and the presence of turbulence suggests that mixing is likely to take place.

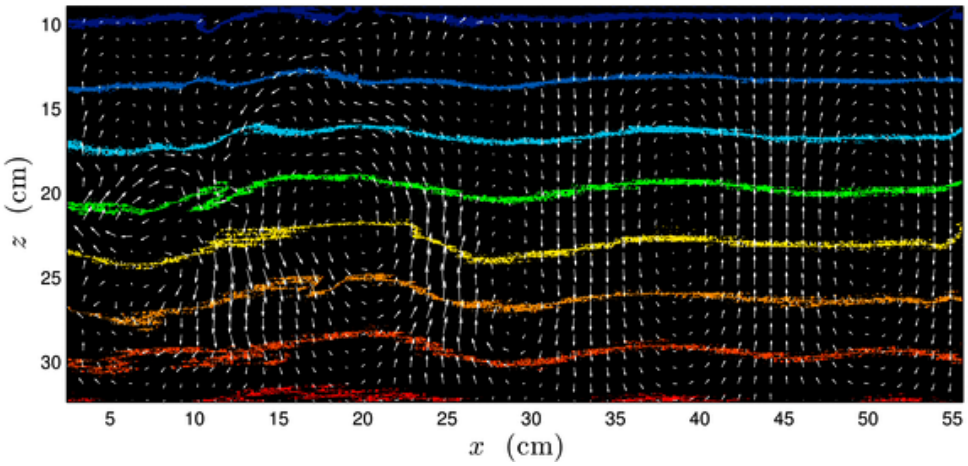

Figure 2: Mixing event observed with the PIV/PLIF set-up. The arrows represent the velocity field, while the colored lines represent selected isopycnals. Experimental parameters: $\omega_0/N = 0.92$, mode-1 plate amplitude: 0.75 cm.

In order to get a more quantitative picture, the simultaneous measurement of density and velocity gives access to quantities based on the correlation between these two fields. For example, the buoyancy flux, defined as $(g/\overline{\rho})\langle\rho' w'\rangle$ where $\langle\cdot\rangle$ stands for the Reynolds average, represents the amount of buoyancy that is transported vertically by the velocity fluctuations, providing turbulent mixing. In oceanic simulations, it is often parameterized using the eddy diffusivity assumption, which assumes a linear relationship between the buoyancy flux and the vertical buoyancy gradient (Chang et al., 2005)

$$\frac{g}{\overline{\rho}}\langle\rho' w'\rangle = K_\mathrm{t} N^2 \ , \tag{1}$$

where K_t is the eddy diffusivity and N the buoyancy frequency. The eddy diffusivity defined above is directly measurable in the present configuration and provides a link between flow dynamics and irreversible turbulent fluxes.

In previous articles (Joubaud et al., 2012; Bourget et al., 2013), we have studied several aspects of Triadic Resonant Instability (TRI) of internal waves, where through non-linear triad resonant interaction, two daughter-waves emerge from a primary wave, with lower frequency and generally smaller wavelength. This process is prone to enhance wave induced mixing, since the shorter wavelengths can lead more easily to overturning and irreversible mixing of the stirred density layers. In addition, oceanographic studies have

also suggested that the TRI process participates in the energy cascade towards mixing (MacKinnon et al., 2013). For this reason, we will evaluate the quantity K_t in cases with and without TRI.

Two experiments exp$A$ and exp$B$ combining simultaneous PLIF and PIV measurements are carried out to investigate the evolution of K_t. The mode-1 plate amplitude is 1 cm in both experiments. In exp$A$, the nondimensional forcing frequency $\omega_A/N = 0.50$ is too low for the experiment to exhibit any TRI instability. On the contrary, in exp$B$ ($\omega_B/N = 0.95$), secondary internal waves issued from the TRI mechanism are expected to develop efficiently (Bourget et al., 2013). Fig. 3 shows subsequent steps of the TRI onset on the velocity field. First, a mode-1 internal wave is radiated from left to right and, later, reflected at the right end wall. After a few forcing periods, ripples superimposed to the linearly propagating normal mode indicate that smaller scale waves are at play. The primary internal wave mode degenerates into a couple of secondary internal wave beams fulfilling the temporal resonance condition for TRI. Towards the end of the experiment they occupy the whole tank. Although PLIF measurements are overall less smooth than PIV measurements, the secondary waves are also observed in the density anomaly field in Fig. 4, left panels, for $t = 9$, 11, 13, 15 and 26 T_0.

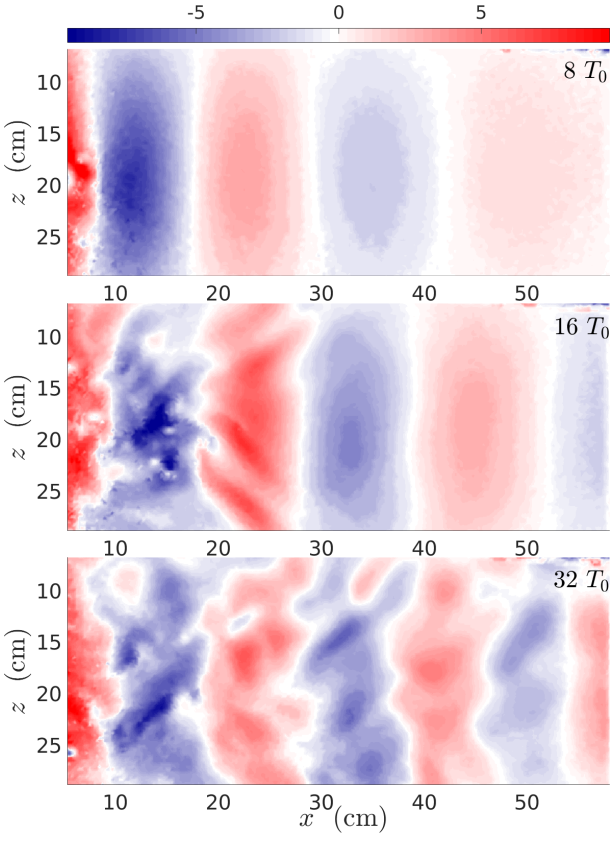

Figure 3: Vertical velocity field $w(x, z, t)$ (mm·s^{-1}) issued from PIV measurements in exp$B$ at $t = 8\ T_0$ (top), $t = 16\ T_0$ (center) and $t = 32\ T_0$ (bottom).

In both experiments, the eddy diffusivity at time t is computed using the average value for $\rho' w'(x, z, t')$ between $t - 2T_0$ and $t + 2T_0$. The impact of the flow dynamics on irreversible energy fluxes shows large differences between exp$A$ and exp$B$. In the former case (not shown), random fluctuations of K_t of the order of 1 mm$^2 \cdot$ s^{-1} are observed, defining the

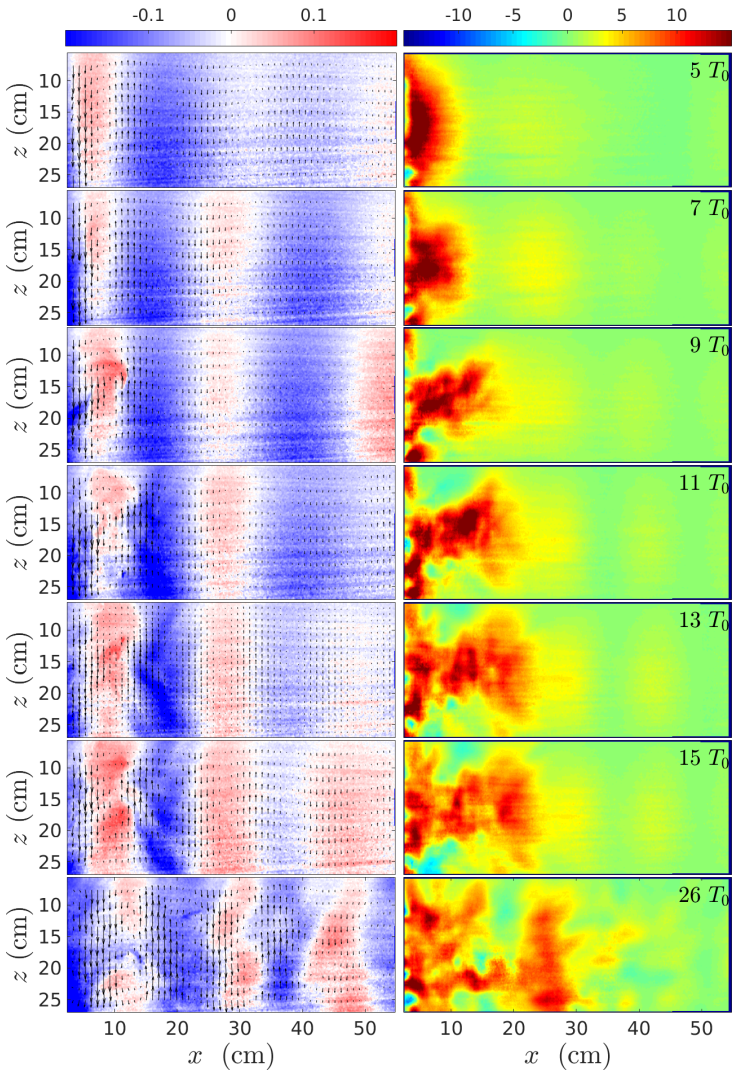

Figure 4: Left panels, from top to bottom: Density anomaly fields $\rho'(x, z, t)$ (in kg·m^{-3}), superimposed with velocity vectors in exp$B$ for t = 5, 7, 9, 11, 13, 15 and 26 T_0. Right panel: Associated turbulent diffusivity fields $K_t(x, z, t)$ (mm^2·s^{-1}). Experimental parameters: $\omega_0/N = 0.95$, mode-1 plate amplitude: 1 cm.

noise level of this measurement. Hence no quantitative positive turbulent buoyancy flux is measured in the configuration of low forcing frequency.

In exp$B$, a steady patch of intense eddy diffusivity with a typical magnitude of 10 to 15 mm$^2 \cdot$s^{-1} is observed (see right panels of Fig. 4). The largest values of K_t in this patch are reached at mid-depth, where the horizontal velocity shear has the largest amplitude. For increasing time, the patch of intense mixing spreads towards the tank interior. The vertical extent of the mixing region increases linearly with the distance to the generator. This vertical spreading matches the propagation of secondary wave beams at constant angles away from their generation zone. After 30 T_0, heterogeneous patches with large K_t values are measured over the whole tank length. Hence, quantitative turbulent buoyancy fluxes are enhanced in the region of TRI. They result in values of K_t at least one order of magnitude larger than the background value measured in the experiment with no TRI. One can conclude that the TRI process participates in the direct energy cascade towards irreversible mixing.

4 Conclusion

Combining PLIF with simultaneous and spatially synchronized velocity measurements via PIV allows for the measurement of correlations between density and velocity fields, and in particular gives access to the eddy diffusivity field K_t. The energy cascade occurring during the TRI process yields values of K_t up to 15 $\mathrm{mm}^2 \cdot \mathrm{s}^{-1}$, which are one order of magnitude larger than the background eddy diffusivity for a linear normal mode propagation. Looking at long term evolution of the density profile, we have also observed that the local mixing evidenced by the K_t measurement converts, during larger duration experiments, into a deformation of the background density profile, highlighting the occurence of irreversible mixing, attesting a gain of potential energy, taken from the internal wave flow kinetic energy. This mixing takes place principally in the middle part of the tank, where the shear of the mode-1 is dominant.

The present values of K_t are obtained in an idealized laboratory scale configuration and cannot be directly used to assess oceanic turbulent diffusivities. However, it is clear that TRI can substantially enhance internal wave induced mixing away from topographies for quasi-linear stratifications. Future experimental studies will involve a full parametric study of the system, and could investigate upon the relation between the dynamics of TRI and induced mixing for non-uniform background stratifications.

References

Bourget, B., Dauxois, T., Joubaud, S., and Odier, P. (2013). Experimental study of parametric subharmonic instability for internal plane waves. *J. Fluid Mech.*, 723:1–20.

Chang, Y. S., Xu, X., Ozgokmen, T. M., Chassignet, E. P., Peters, H., and Fischer, P. F. (2005). Comparison of gravity current mixing parameterizations and calibration using a high-resolution 3d nonhydrostatic spectral element model. *Ocean Model.*, 10:342–368.

Dossmann, Y., Bourget, B., Brouzet, C., Dauxois, T., Joubaud, S., and Odier, P. (2016). Mixing by internal waves quantified using combined PIV/PLIF technique. *Experiments in Fluids*, in press.

Garrett, C. and Kunze, E. (2007). Internal tide generation in the deep ocean. *Annu. Rev. Fluid Mech.*, 39:57–87.

Gostiaux, L., Didelle, H., Mercier, S., and Dauxois, T. (2007). A novel internal waves generator. *Experiments in Fluids*, 42(1):123–130.

Hjertager, L. K., Hjertager, B. H., Deen, N. G., and Solberg, T. (2003). Measurement of turbulent mixing in a confined wake flow using combined PIV and PLIF. *Can. J. Chem. Eng.*, 81:1149–1158.

Hu, H., Kobayashi, T., Segawa, S., and Taniguchi, N. (2000). Particle image velocimetry and planar laser-induced fluorescence measurements on lobed jet mixing flows. *Exp. Fluids*, Suppl.:S141–S157.

Joubaud, S., Munroe, J., Odier, P., and Dauxois, T. (2012). Experimental parametric subharmonic instability in stratified fluids. *Phys. Fluids*, 24(4):041703.

Kunze, E. and Smith, S. (2004). The role of small-scale topography in turbulent mixing of the global ocean. *Oceanography*, 17(1):55–64.

Lamb, K. G. (2014). Internal Wave Breaking and Dissipation Mechanisms on the Continental Slope/Shelf. *Annu. Rev. Fluid Mech.*, 46:231–254.

MacKinnon, J. A., Alford, M. H., Sun, O., Pinkel, R., Zhao, Z., and Klymak, J. (2013). Parametric subharmonic instability of the internal tide at 29 n. *J. Phys. Oceanogr.*, 43(1):17–28.

Munk, W. and Wunsch, C. (1998). Abyssal recipes ii: energetics of tidal and wind mixing. *Deep Sea Res. Part 1 Oceanogr. Res. Pap.*, 45(12):1977 – 2010.

Odier, P., Chen, J., and Ecke, R. E. (2014). Entrainment and mixing in a laboratory model of oceanic overflow. *J. Fluid Mech.*, 746:498–535.

Staquet, C. and Sommeria, J. (2002). Internal gravity waves: From instabilities to turbulence. *Annu. Rev. Fluid Mech.*, 34:559–593.

Troy, C. and Koseff, J. (2005). The generation and quantitative visualization of breaking internal waves. *Exp. Fluids*, 38(5):549–562.

Wunsch, C. and Ferrari, R. (2004). Vertical mixing, energy and thegeneral circulation of the oceans. *Annu. Rev. Fluid Mech.*, 36:281–314.